OBSERVATION OF GROUND STRAIN IN OSAKA BASIN FOR THE SEISMIC DESIGN OF BURIED PIPELINE

Nima MOHAMMADI [1] and Yasuko KUWATA[2]

[1]Non-member of JSCE, Dept. of Civil Eng., Graduate School of Engineering, Kobe University
(Rokkodai 1-1, Nada-ku, Kobe 657-8501, Japan)
E-mail: 207t753t@stu.kobe-u.ac.jp
[2]Member of JSCE, Associate Professor, Dept. of Civil Eng., Graduate School of Engineering, Kobe University
(Rokkodai 1-1, Nada-ku, Kobe 657-8501, Japan)
E-mail: kuwata@kobe-u.ac.jp (Corresponding Author)

In the guidelines for seismic design of buried pipelines, the ground strain due to seismic wave motion, which is calculated by dividing the wave velocity by the wave propagation velocity, is used as acting external force. However, the seismic design guidelines for buried water pipelines in Japan and the United States show a difference of more than 10 times in the value of the propagation velocity. In this study, we clarify the characteristics of ground strain due to seismic motion from earthquake records obtained by a strong-motion observation array installed in Fukushima, Osaka City. From the observed records with moderate seismic motion, the peak ground velocity and maximum strain indicated that the apparent wave propagation velocity was more than 2 km/s.

Key Words : *ground strain, seismic design of buried pipeline, wave propagation, observation*

1. INTRODUCTION

The seismic calculation method for buried pipe-lines caused by seismic waves in the seismic design guideline of water works in Japan (hereinafter referred to as "JWWA Guidelines") has not been significantly changed since its introduction in 1979, when the response displacement method was introduced for the first time, except for adding the external forces due to the introduction of L2 seismic motion in 1997. The method has long followed the concept of the Oil Pipeline Design Standard, which was the first to introduce the response displacement method in Japan. Basically, the action is the ground strain due to seismic ground motion calculated by dividing the wave velocity by the velocity of wave propagation. The ground strain calculated by the JWWA guideline is considered to be larger based on the comparison with previous studies on strain observation and other seismic design guidelines. In this study, the characteristics of ground strain due to seismic ground motion were clarified based on seismic records from a strong-motion observation array installed in Fukushima, Osaka City.

2. GROUND STRAIN IN SEISMIC DESIGN GUIDELINES

According to the JWWA guidelines, the ground strain due to the seismic ground motion, ε, is calculated from the maximum displacement, U_h, and the wavelength of shear wave, L.

$$\varepsilon = \pi \cdot U_h / L \tag{1}$$

The maximum displacement is obtained from the response velocity spectrum. The harmonic mean of the shear wave wavelengths of the surface sediment and the engineering baserock is the wavelength of the shear wave propagation, when the surface sediment is considered to be excited in the first-order shear mode. Furthermore, referring to the ground profiles exemplified in the guideline, the S-wave velocity of the surface sediment is Vs= 70 m/s, and the S-wave velocity of the engineering baserock is Vs = 300 m/s. Therefore, the harmonic mean of shear wave velocity is around 130 m/s, depending on the layer thickness of the surface sediments. Using the profile of the model ground in the JWWA guidelines, the ground strain is calculated to be 6.0×10^{-4} for the Level 1

earthquake motion and 5.0×10^{-3} for the Level 2 earthquake motion.

On the other hand, the ground strain, ε_{max}, in the ALA guideline is calculated from the peak velocity of ground surface, *PGV* divided by the wave propagation velocity *C*.

$$\varepsilon_{max} = PGV/C \quad (2)$$

The propagation velocity, *C*, is assumed to be the velocity of the body wave, *C* = 3.9 km/s shown in the calculation example. The ground strains can be calculated to be 9.0×10^{-5} to 3.0×10^{-4} in the range that the *PGV* is 12 to 120 cm/s. Therefore, the ground strains calculated in the JWWA guideline is about 10 times larger than those in the ALA guidelines, even assuming *PGV*=100 cm/s in the ALA guideline is the same level as the JWWA guideline.

Mizuno et al. [3] installed several seismometers in the tunnel to measure seismic ground strain, and reported that the strains observed during two earthquakes with M_j 6.8 were about 4.0×10^{-6}. Furthermore, for the earthquake with a larger magnitude, the maximum strain was recorded with a delay relative to the peak of seismic velocity. The propagation velocity of the body wave is 3.8 km/s, which is slower than the apparent propagation velocity in the normal direction. Sato et al.[4] also conducted buried pipe strain observations in Chiba, and reported a maximum pipe strain of 18.8×10^{-6} for an earthquake with M_j 6.1 and an epicenter distance of 28 km. Based on these observations, it can be said that the ground strain calculated by the JWWA guidelines is large.

3. OBSERVATION OUTLINE

(1) Osaka Basin

The Osaka basin is surrounded by the Hokusetsu mountains to the north, the Ikoma and Kongo mountains to the east, the Izumi mountains to the south, and Osaka bay to the west, and is a low-lying plain with a nearly elliptical shape measuring about 55 km in the northeast-southwest direction and about 28 km in the northwest-southwest direction. Figure 1 shows the microtopographic classification of the Osaka basin based on the J-SHIS[5] and the locations of seismic stations of K-NET[6], KiK-net[6], and CEORKA[7]. The Osaka basin consists mainly of alluvial lowlands, and the surrounding mountains are composed of granitic rocks that form the bedrock of the Osaka basin. the Osaka Formations develop hills of about 200 m in elevation between the mountains. In addition, unconsolidated sediment layers up to 3,000 m in depth are distributed beneath the basin.

Miyakoshi et al.[8, 9] obtained average predominant periods from slightly long-period seismic motions of the earthquakes with M_j5 or more observed at strong-motion stations of the CEORKA, and found that the horizontal waves have a predominant period of 2 to 6 s and the vertical waves have the predominant period of 1 to 3 s. Furthermore, the predominant periods of a surface wave obtained from the dispersion curves of Rayleigh and Love waves are harmonic to these periods. The harmonic relationship between the natural periods of the Rayleigh and Love waves and the predominant periods of the surface waves indicates that the slightly long-period seismic motions provoked in the Osaka basin are mainly surface waves. Referring to the microtopographic classification in Figure 1, the predominant period is 4 to 6 s on the gravelly plateau in the central part of the Osaka basin, 6 to 8 s on the delta and coastal lowlands slightly to the west such as FKS, and 8 to 10 s on the reclaimed land around Osaka bay such as OSKH02 further to the west. In the fan-shaped area on the east side of the Osaka basin, Rayleigh waves are predominant with a period of 8 to 10 seconds. On the other hand, Rayleigh waves have a similar period to that of Love waves, but their period is about half that of Love waves.

(2) Seismometers location

Three seismometers were set around the Fukushima station (FKS) of the CEORKA, where significant surface waves have been observed during earthquakes in previous studies, and started seismic observations in 2017. Figure 2 shows the locations of the seismometers around FKS; OSA and OSB were installed in the warehouses of Fukushima Elementary School and

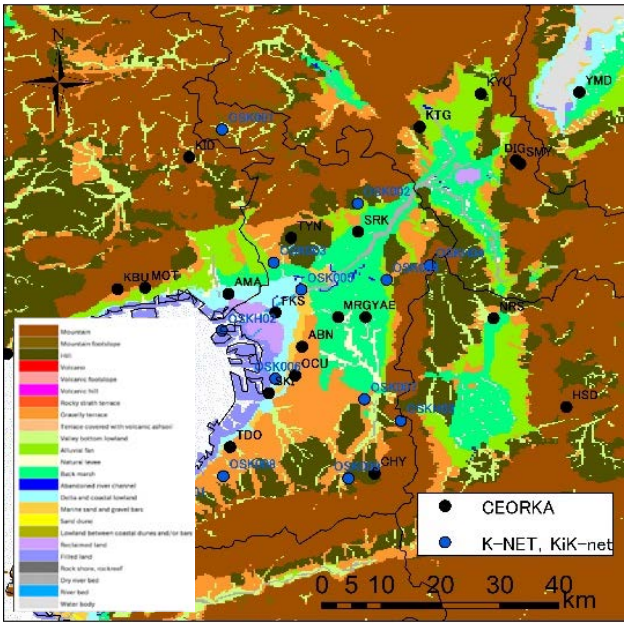

Fig.1 Microtopographic classification map of the Osaka basin and observation point locations.

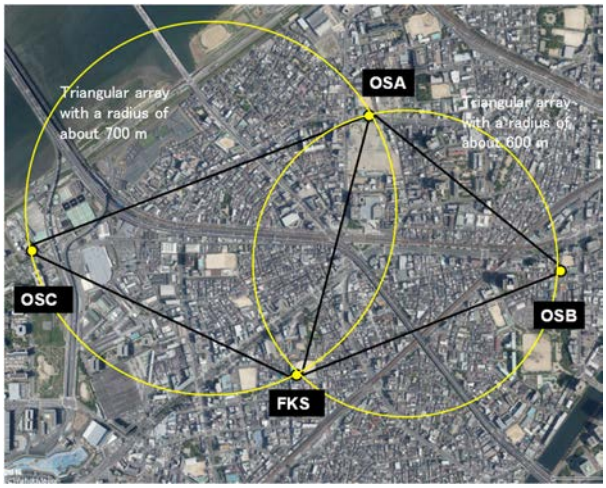

Fig.2 Location of seismographs.

(a) OSA (b) OSB

(c)OSC

Fig.3 Seismograph equipment. (a) OSA, (b) OSB and (c) OSC stations.

Table 1 Seismograph locations

	Latitude(deg.)	Longitude (deg.)
OSA	34.69848	135.4758
OSB	34.69336	135.4832
OSC	34.69427	135.4623
OSC2	34.67796	135.4211
FKS	34.69003	135.4732

OSC was moved to OSC2 after December 2021.

Ebie Higashi Elementary School, respectively, and OSC was installed in the Ebie Sewage Treatment Plant. The OSA and OSB were installed in a triangular array with a radius of about 600 m, and the OSC, OSB, and FKS were installed in a triangular array with a radius of about 700 m. The OSA and OSB began observations in September 2017, and the OSC began observations in October 2017. The OSA and OSB began observations in September 2017, and the OSC began observations in October 2017. In December 2021, the OSC was relocated 4 km west of the location shown in Figure 1 to continue observations.

Table 2 Seismograph specifications

Model	CV-910
Mesurement frquency range	0.025-70 Hz
Detector type	Servo type velocity meter (VSE-11)
Number of record components	9 components (of which, 3 components of acceleration)
Maximum recording range	±1000 gal
AD conversion resoltion	16 bit
Sampling frequency	100 Hz
Time adjustment	Automatic adjustment by GPS
External dimensions	474(W)×302(D)×260(H) mm

Table 2 shows the specifications of three seismometers used in this study. The seismograph used in this study was a CV-910 velocity seismograph (Tokyo Sokuhin Co.). The detector is a servo velocity meter (VSE-11) and the sampling frequency is set at 100 Hz. A new logger manufactured by aLab Inc. was installed externally and synchronized with GPS. 24-hour continuous observation records were sent to a server via a network every minute, allowing real-time observation.

Since the installation of the seismographs, the H/V spectral ratios were compared day and night to see if there were any effects of noise from renovation work in the elementary school or operation of pumps in the sewage treatment plant[10]. Predominant periods of 1 second or less showed a maximum difference of about 0.1 s even at the same site. However, the influence of noise in the short period due to mechanical vibration from construction, pumps, etc. was not significant. The nighttime H/V spectral ratios indicated predominant at 0.6 to 0.7s. The N values were referred from the geotechnical profiles in a 250 x 250 m mesh model from the KG-NET/Kansai Geotechnical Network's Geotechnical Library of the Kansai Region. The natural period of the surface ground was calculated according to the specifications for road bridges. The results are consistent with the natural period of the sediment above the engineering bedrock. Depending on the time of observation, some of the H/V spectral ratios were also observed to be predominant at 2 to 3 s, which is the natural period of the slightly deep ground structure in the Osaka basin.

4. OBSERVATION RESULT

(1) Records used in this study

In this study, we organized the earthquake records by

Table 3 List of strong motion records used in this study

Event No.	Date	Event Time	Epicenter		Depth (km)	Mj	PGV NS comp. (cm/s)				PGV EW comp. (cm/s)			
			Latitude	Longitude			OSA	OSB	OSC	FKS	OSA	OSB	OSC	FKS
1	2018.06.18	7:57	34.84N	135.62E	13	6.1	13.56	14.03	7.14	10.10	26.93	25.35	24.23	18.19
2	2018.06.19	0:30	34.86N	135.61E	10	4.1	0.15	0.18	0.17	0.10	0.39	0.26	0.28	0.17
3	2018.06.19	4:52	34.84N	135.62E	13	3.9	0.11	0.13	0.09	0.07	0.23	0.13	0.17	0.08
4	2018.06.19	7:51	34.84N	135.61E	11	3.9	0.26	0.17	0.13	0.13	0.44	0.32	0.33	0.23
5	2018.11.02	16:54	33.70N	135.19E	44	5.4	0.28	0.27	0.35	0.30	0.30	0.29	0.25	0.22
6	2019.03.13	13:49	33.80N	134.91E	43	5.3	0.60	0.80	0.38	0.37	0.91	0.85	0.79	0.48
7	2021.02.13	23:08	37.73N	141.70E	55	7.3	0.73	0.64	*	0.72	0.79	0.44	*	0.68
8	2021.12.03	9:27	33.80N	135.15E	18	5.4	0.73	0.53	0.48	0.29	0.63	0.65	0.45	0.43
9	2022.01.22	1:08	32.72N	132.07E	45	6.6	0.76	0.92	0.88	0.65	0.72	1.01	0.89	0.71
10	2022.03.11	17:59	35.19N	135.10E	15	4.1	0.27	0.25	*	0.20	0.19	0.14	*	0.14
11	2022.03.16	23:36	37.70N	141.62E	57	7.4	1.00	1.12	*	1.16	1.20	1.19	*	1.20
12	2022.03.31	23:34	35.05N	135.56E	13	4.4	0.13	0.15	0.13	0.13	0.40	0.30	0.32	0.27
13	2022.04.03	18:58	34.91N	135.63E	11	3.9	0.11	0.07	0.06	0.07	0.12	0.10	0.06	0.06
14	2022.04.13	11:12	35.04N	135.57E	13	3.9	0.05	0.08	0.10	0.06	0.12	0.07	0.15	0.06
15	2022.04.25	13:10	35.04N	135.58E	14	4.1	0.09	0.11	0.08	0.08	0.12	0.08	0.08	0.06
16	2022.04.30	18:06	35.05N	135.56E	12	4.3	0.17	0.15	0.12	0.16	0.15	0.12	0.16	0.08
17	2022.05.02	22:21	35.05N	135.57E	13	4.4	0.12	0.13	0.14	0.12	0.10	0.07	0.15	0.07

Note) Symbol * indicates measurement failure.

following the procedure. The earthquakes with seismic intensity on the JMA scale is 1 or more in Osaka were selected, and among them, PGV at the station is 0.1 cm/s or more are used starting from the earthquake in northern Osaka in 2018. Table 3 shows the list of earthquakes, whose records is used in this study. Figure 4 shows the map of the earthquake epicenter, in which the number is the same as the event number in Table 3. The records of 17 earthquake events were analyzed. Events No. 1 to No.4 are the main shock and aftershocks in the northern part of Osaka Prefecture in 2018. Three earthquakes area off Wakayama prefecture. Events No. 13 to 17 are the earthquake that frequently occurred near Kyoto prefecture. As for far earthquakes, the 2021 off Fukushima earthquake (No.7), the 2022 off Fukushima earthquake (No.11), and the 2022 Hyuga Nada earthquake (No.9) are also included[12].

(2) Semblance analysis

In analyzing the propagation characteristics of these observed waves, we performed semblance analysis[13] results for each of the two horizontal components of velocity. The results on the earthquake of northern Osaka in 2018 were previously reported[14]. The propagation velocities of the waves during the time of predominance of the body waves were 4 to 8 km/s occurring from the source direction for all earthquakes. The propagation velocities of the subsequent waves, which are considered to be caused by surface waves, were in the range of 0.4 to 1.0 km/s, and the incident direction was not constant with time. Here, the results of semblance analysis are not described in detail.

Fig.4 Epicenter of the earthquake whose seismic records used in this study. The number in this figure corresponds to the event number in Table 3.

(3) Stain along observation line between stations

The characteristics of ground strain due to seismic ground motion were analyzed by calculating the strain of two observation axes of the high-density observation network. The dense observation network enables to evaluate the normal strain by two-point displacement appropriately. We calculated the normal strain along the observation line by dividing the displacement difference between two arrayed points, using Eq. (3).

$$\varepsilon_{mn}(t) = \{X_n(t) - X_m(t)\}/L_{nm} \qquad (3)$$

Where, $X_i(t)$ is the displacement of observation station i, and L_{nm} is the distance of the observation line at stations n and m.

The displacement data from the observed records was obtained by the integration with bandpass 0.1 to 10.0 Hz.

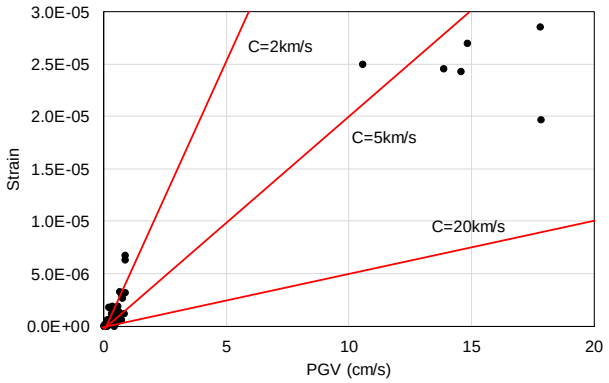

Fig.5 Relationship between PGV and maximum strain for all earthquakes.

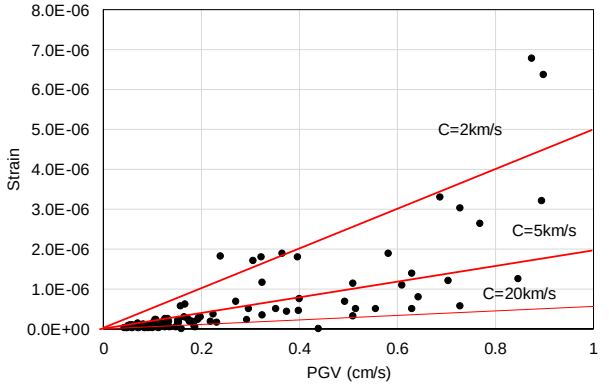

Fig.6 Relationship between PGV and maximum strain under PGV = 1 cm/s.

The relationship between the normal strain along each of these observation lines and the PGV for all earthquake as shown in Figure 5. The PGV on the horizontal axis is the average of the peak velocities in the line direction between two stations, and the vertical axis indicates the maximum normal strain in the line direction. Since the velocities are less than 1 cm/s except for event No. 1 which was about 20 cm/s recorded in the stations, Figure 6 shows the relationship excluding the record of event No. 1. Note that the time of average PGV and the time of maximum strain are not always same. By the way, the conventional method to estimate the maximum strain under an earthquake is expected for the future. The relationship with PGV seems to be easy to estimate. The maximum strains are from 2.0×10^{-5} to 3.0×10^{-5} for event No. 1, and they are less than 7.0×10^{-6} for the other events. These maximum strains are similar to those in the previous studies[3),4)].

The apparent wave propagation velocity is shown in the figures from Eq.(2). The apparent wave propagation velocity was nearly 5 km/s for event No. 1, and it was distributed in the range of 2 to 20 km/s for the other earthquakes. However it was never less than 1 km/s as in the JWWA guideline.

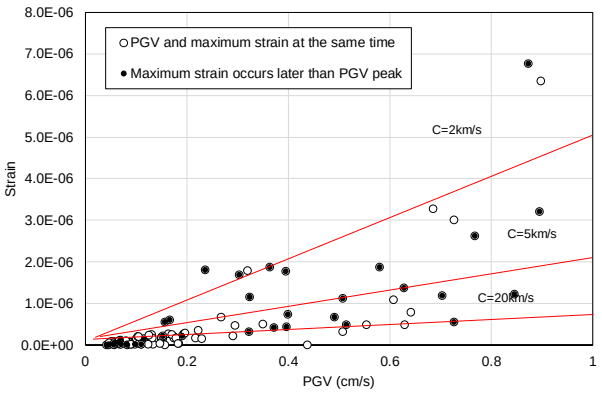

Fig.7 Relationship between PGV and maximum strain for the record less than 1 cm/s in PGV.

The records where the maximum strain occurred more than 5 s later than the PGV time are indicated by black circles in Figure 7. In the case of earth quakes with epicenters in Wakayama, Fukushima-Oki, and Hyuga-nada with epicenter distances of 100 km or more, the maximum strain occurred later than the time of PGV, suggesting that the strain was caused by surface waves. In the case of the maximum strain due to surface waves, the propagation velocity itself is less than 1 km/s, but the velocity at that time is half that of the PGV. As a result, the strain falls within the distribution area shown in the figures.

The strain calculated from the observation results is much smaller than the value calculated by the JWWA guidelines. The apparent wave propagation velocity was more than 2 km/s. It is necessary to clarify the relationship between PGV and maximum strain for large earthquakes in the future.

6. CONCLUSIVE REMARKS

In this study, the characteristics of ground strain due to seismic ground motion were clarified based on seismic records from a strong-motion observation array installed in Fukushima, Osaka. The following can be summarized as conclusions.

- Characteristics of ground strain due to seismic waves were analyzed from the strain of two observation point axes of the high-density observation network.
- The maximum strains are from 2.0×10^{-5} to 3.0×10^{-5} for the earthquake with M_j 6.1, and they are less than 7.0×10^{-6} for the other events. Those values of maximum strain are similar to those in the previous studies.
- The apparent wave propagation velocity for the records with the PGV = 1 cm/s or less was more than 2 km/s.

- When ground strain was examined in Osaka, it was found that ground strain due to surface waves was outstanding if the epicenter distance was more than 100 km.
- Among the data analyzed in this study, in the event of an earthquake with an epicenter distance of 100 km or more off the coast of Wakayama, Fukushima, and Hyuga Nada, the maximum strain will occur later than the time of PGV generation. Which is conceivable that it is a distortion due to surface waves.

ACKNOWLEDGMENT: We would like to express our gratitude to the Committee of Earthquake Observation and Research in the Kansai Area (CEORKA) for the use of their strong-motion records in conducting this study. We would like to express special acknowledgment to Associate Professor, Hiroyuki Goto, DPRI, Kyoto University, for supporting observation setting and technical advices in this study.

REFERENCES

1) Japan Water Works Association: Seismic Design Guideline of Water Works,1997,1999. (in Japanese)
2) American Lifeline Alliance: Seismic Guidelines for Water Pipelines, 2005.
3) Mizuno, K., Ohmachi, T., Inoue, S.: Study of seismic strain in tunnels located in shallow ground, Annual Meeting of JSCE, 2008. (in Japanese)
4) Sato, N., Katayama, T., Nakamura, M., Iwamoto, T., Ohbo, N.: A study on behavior of ground strain and buried pipe strain during earthquake, Proc. of the JSCE Earthquake Engineeing Symposium, Vol.19, pp. 21-24, 1987. (in Japanese)
5) National Research Institute for Earth Science and Disaster Resilience (NIED): Japan Seismic Hazard Information Station (J-SHIS) (http://www.j-shis.bosai.go.jp/)
6) National Research Institute for Earth Science and Disaster Resilience (NIED): Strong-motion seismograh networks (K-NET, KiK-net(https://www.kyoshin.bosai.go.jp/)
7) The Committee of Earthquake Observation and Research in the Kansai Area (CEORKA): Strong ground motion records (http://www.ceorka.org/)
8) Miyakoshi,K., Horike, M.: Predominant period of the long-period ground motions in the Osaka basin, Butsuri-Tansa (Geophysical Exploration), Vol. 59, Issue 4, pp. 327-336, 2006 (in Japanese)
9) Miyakoshi, K., Onishi, Y., Akazawa, T., Horike, M.:Predominant period for surface waves based on the Osaka basin model, Geophysical bulletin of Hokkaido University, Vol.69, pp.41-50, 2006 (in Japanese)
10) Mizukami, M., Kuwata, Y., Goto, H., Fukushima, Y.: Development of a high-density seismic observation system in the Osaka Plain, JSCE Kansai Branch Annual Meeting, 2018 (in Japanese)
11) Kansai Geo-informatics Network (KG-NET): Library of Kansai Geo-Information (URL: https://www.kg-net2005.jp/index/lib.html)
12) Japan Meteorological Agency Earthquake information, Detail information Issued on 2022/03/16 15:11", 16 March 2022. Archived from the original on 16 March 2022. Retrieved 16 March 2022.
13) Neidell, N.S. and Turhantaner, M. : Semblance and other coherency measures for multichannel data, Geophysics, Vol.36, No.3, pp.482-497, 1971.
14) Kuwata, Y., Komatsu, H: Seismic characteristics of surface waves in the Osaka Plain during the earthquake in the northern part of Osaka Prefecture, JSCE Kansai Branch Annual Meeting, 2019 (in Japanese)